New constraints on ocean carbon

Deliverable D1.6

Authors: Peter Landschützer, Nicolas Gruber, Jens D. Müller, Lydia Keppler, Luke Gregor

This project received funding from the Horizon 2020 programme under the grant agreement No. 821003.

Document Information

GRANT AGREEMENT	821003
PROJECT TITLE	Climate Carbon Interactions in the Current Century
PROJECT ACRONYM	4C
PROJECT START DATE	1/6/2019
RELATED WORK PACKAGE	W1
RELATED TASK(S)	T1.2.1, T1.2.2
LEAD ORGANIZATION	MPG
AUTHORS	P. Landschützer, N. Gruber, J.D. Müller, L. Keppler and L. Gregor
SUBMISSION DATE	x
DISSEMINATION LEVEL	PU / CO / DE

History

DATE	SUBMITTED BY	REVIEWED BY	VISION (NOTES)
18.11.2020	Peter Landschützet (MPG)	P. Friedlingstein (UNEXE)	

Please cite this report as: P. Landschützer, N. Gruber, J.D. Müller, L. Keppler and L. Gregor, (2020), New constraints on ocean carbon, D1.6 of the 4C project

Disclaimer: The content of this deliverable reflects only the author's view. The European Commission is not responsible for any use that may be made of the information it contains.

Table of Contents

List of figures

About 4C

Climate-Carbon Interactions in the Coming Century (4C) is an EU-funded H2020 project that addresses the crucial knowledge gap in the climate sensitivity to carbon dioxide emissions, by reducing the uncertainty in our quantitative understanding of carbon-climate interactions and feedbacks. This will be achieved through innovative integration of models and observations, providing new constraints on modelled carbon-climate interactions and climate projections, and supporting Intergovernmental Panel on Climate Change (IPCC) assessments and policy objectives.

Executive Summary

This deliverable describes four data-based products on the air-sea CO_2 exchange and the dissolved carbon content in the ocean interior. Two of the products describe updates of existing products, namely for surface CO_2 fluxes (MPI-SOMFFN and the advanced MPI-ULB-SOMFFN-clim) and interior accumulation of anthropogenic carbon (based on eMLR(C*)). In addition, one new constraint on surface CO_2 fluxes, as well as other carbon system parameters at the sea surface, is presented, namely the OceanSODA-ETHZ product and a new constraint on the seasonal through interannual variability of the dissolved inorganic carbon (DIC) pool in the interior ocean (MOBO-DIC_MPIM). The different products highlight the exceptional advances made within the 4C project to provide new constraints on the ocean carbon cycle based on observations of the sea surface partial pressure of CO_2 (pCO_2) and DIC measurements from the repeat hydrography programs, i.e., two independent data sources. All data products presented in this deliverable report are freely accessible (see respective “data availability” section) and serve as novel constraints for the partner work packages within the 4C project.

Keywords

Ocean, carbon, air-sea CO2 fluxes, carbon storage, anthropogenic carbon

2 New observation-based constraints on the surface ocean carbonate system and the air-sea CO2 flux

2.1 OceanSODA-ETHZ

The Satellite Oceanographic Dataset for Acidification by ETH Zürich (OceanSODA-ETHZ) represents a newly developed product describing the global-scale evolution of the surface marine carbonate system over the period 1985 through 2018 [Gregor and Gruber, 2020]. Concretely, OceanSODA-ETHZ contains global 1°x1° and monthly estimates of surface ocean pCO_2, total alkalinity (TA), dissolved inorganic carbon, pH, and aragonite saturation amongst other variables of the marine carbonate system. The availability of not only pCO_2, but also TA and DIC allow for the attribution of changes in the pCO_2 and thus air-sea pCO_2 fluxes.

2.1.1 Observations

For pCO_2, the gridded product from the Surface Ocean CO_2 Atlas is used (SOCAT, [Sabine et al. 2013; Bakker et al. 2016]). Bottle samples of TA from the Global Ocean Data Analysis Project (GLODAPv2 [Olsen et al. 2019, Olsen et al. 2020]) are used to train the regression algorithm. TA is limited to the upper 20 m and 30 m in the tropics and high latitudes respectively [Lee et al. 2006]. Surface ocean variables that are proxies for pCO_2 and TA are used as predictors; these include sea surface temperature, satellite chlorophyll, surface salinity from model assimilations, climatological MLD from Argo, and climatological nutrient observations. A subset of these are also required to calculate the remaining parameters of the marine carbonate system.

2.1.2 Method

At the core of the OceanSODA-ETHZ dataset are pCO_2 and TA that are estimated using the Geospatial Random Cluster Ensemble Regression (GRaCER) method [Gregor and Gruber 2020]. This method is similar to the two-step cluster-regression approach used by the SOM-FFN approach of Landschützer et al. [2013] with the addition of an ensemble step. In the first step, the data are grouped with K-means clustering into biogeochemical provinces based on the climatologies of surface ocean variables. We select 16 clusters for TA and 21 clusters for pCO_2. In the second step, pCO_2 or TA are predicted in each cluster using a regression algorithm. For pCO_2 both a feed forward neural network and gradient boosted regression are used (eight ensemble members each), and for TA support vector regression with 16 ensemble members. GRaCER repeats the first two steps to create an ensemble of estimates, where variability achieved through the intrinsic variability of the clustering step as well as the regression approach. The resulting pCO_2 and TA are passed through the *PyCO2SYS* software that calculates the remaining parameters of the marine carbonate system.

2.1.3 Results

The air-sea CO_2 fluxes for OceanSODA-ETHZ range between -1.1 Pg C yr^{-1} in 1990 to -2.4 Pg C yr^{-1} in 2018 without accounting for the input of carbon by rivers. This compares well with other pCO_2-based flux products (Figure 1e) where the ensemble average is -1.3 ± 0.4 Pg C yr^{-1} in 1990 and -2.4 ± 0.4 Pg C yr^{-1} in 2018. Estimates prior to 1988 are the lowest in the ensemble. When adding the riverine carbon input to the OceanSODA-ETHZ estimates, the oceanic uptake for the year 2018 increases to between -2.85 and -3.18 Pg C yr^{-1} assuming an adjustment of either -0.45 or -0.78 PgC yr^{-1} as estimated by Jacobson et al. [2007] and Resplandy et al. [2018], respectively. This adjustment makes the estimates comparable with the Global Carbon Budget [Friedlingstein et al 2019] flux estimates for 2018, 2.6 ± 0.6 PgC yr^{-1}. The OceanSODA-ETHZ flux estimates thus sit at the upper bounds of the oceanic uptake suggested by the GCB. Another comparison can be made with the anthropogenic CO_2 storage change estimates of Gruber et al. [2019] for the period 1994 to 2007, and the update of that estimate for the period 2008 through 2015 (see below). Gruber et al. [2019] estimated an average oceanic uptake of -2.6 ± 0.3 PgC yr^{-1} over the 1994 through 2007 period. Using the larger river adjustment of -0.65 Pg C yr-1, the average annual uptake of OceanSODA-ETHZ over this period is -2.11 PgC yr^{-1}, at the lower end of the range. However, the two estimates are not pertaining to the same quantity. While the ocean interior estimate includes only the accumulation of anthropogenic CO2, the surface fluxes include also the anomalous flux of the natural CO2. Over the period 1994 through 2007, the ocean likely lost some of this natural CO2, perhaps at a rate of 0.2 Pg C yr-1 or so. If this was indeed the case, the ocean interior constraints and the surface one would be in excellent agreement. For the 2008 through 2015 period, the ocean interior estimate is amounts to -3.0±0.3 Pg C yr^{-1}, which is in excellent agreement with the surface ocean constraint from the OceanSODA-ETHZ flux product.

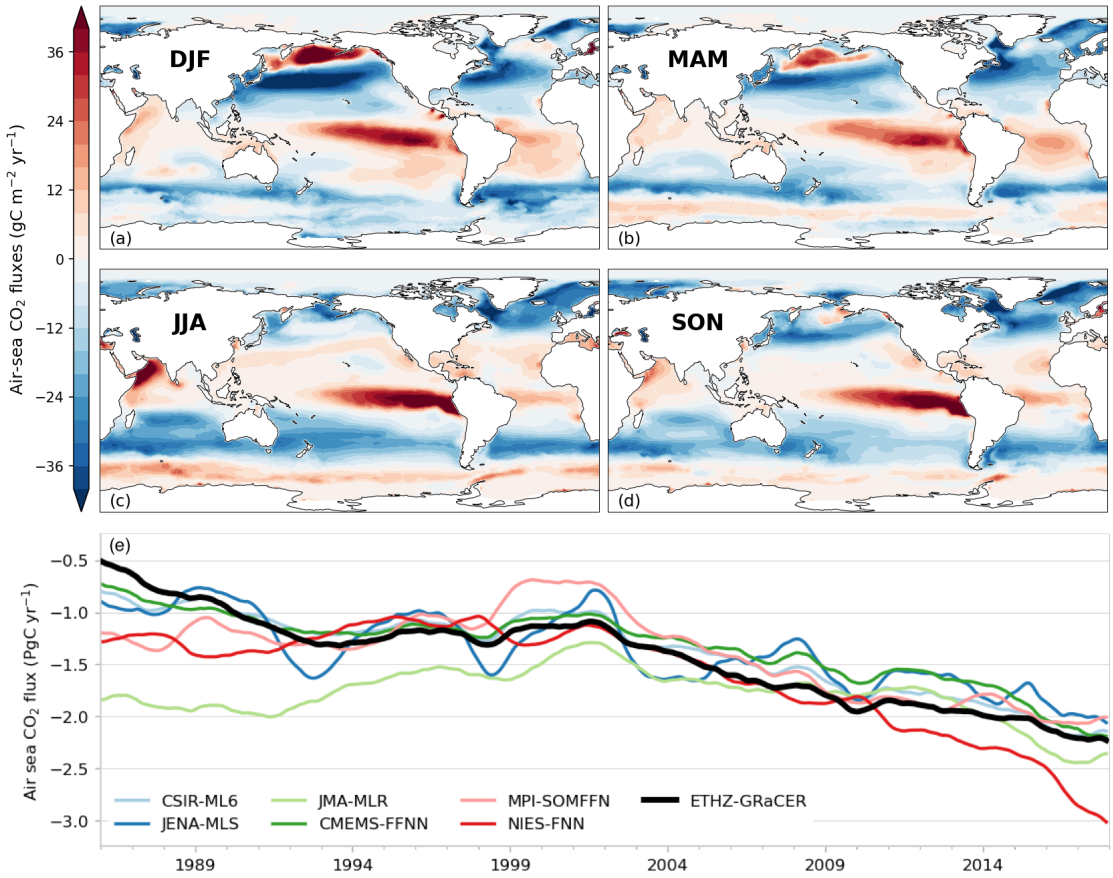

Figure 1: (a-d) seasonal climatologies for air-sea CO_2 fluxes ETH-GRaCER pCO_2 for (a) December, January, February; (b) March, April, May; (c) June, July, August; (d) September, October, November. (e) Spatially integrated air-sea CO_2 fluxes for ETH-GRaCER with fluxes from six published and maintained surface pCO_2 products. All fluxes have been calculated using a standardized approach with consistent solubility and gas transfer velocity.

2.1.4 Data availability

The OceanSODA-ETHZ product is currently under review in ESSD discussions and data can be downloaded at https://doi.org/10.25921/m5wx-ja34. The fluxes are not available in this file but can be requested. Contact Luke Gregor: luke.gregor@usys.ethz.ch.

2.1.5 References

Bakker, D. C. E., et al.: A multidecade record of high-quality fCO2 data in version 3 of the Surface Ocean CO2 Atlas (SOCAT), Earth Syst. Sci. Data, 8, 383– 413, https://doi.org/10.5194/essd-8-383 2016, 2016.

Friedlingstein, P., et al (2019). Global carbon budget 2019. *Earth System Science Data*, *11*(4), 1783–1838. https://doi.org/10.5194/essd-11-1783-2019

Gregor, L. and Gruber, N.: OceanSODA-ETHZ: A global gridded data set of the surface ocean carbonate system for seasonal to decadal studies of ocean acidification, Earth Syst. Sci. Data Discuss., https://doi.org/10.5194/essd-2020-300, in review, 2020

Gruber, N., Clement, D., Carter, B. R., Feely, R. A., van Heuven, S., Hoppema, M., et al.: The oceanic sink for anthropogenic co2 from1994 to 2007. Science, 363, 1193–1199. doi: 10.1126/science.aau5153, 2019

Jacobson, A. R., Fletcher, S. E. M., Gruber, N., Sarmiento, J. L., & Gloor, M. (2007). A joint atmosphere-ocean inversion for surface fluxes of carbon dioxide: 1. Methods and global-scale fluxes. *Global Biogeochemical Cycles*, *21*(1). https://doi.org/10.1029/2005GB002556

Landschützer, P., Gruber, N., Bakker, D. C. E., Schuster, U., Nakaoka, S., Payne, M. R., Sasse, T. P., and Zeng, J.: A neural network-based estimate of the seasonal to inter-annual variability of the Atlantic Ocean carbon sink, Biogeosciences, 10, 7793–7815, https://doi.org/10.5194/bg-10-7793-2013, 2013

Lee, K., Tong, L. T., Millero, F. J., Sabine, C. L., Dickson, A. G., Goyet, C., Park, G.-H., Wanninkhof, R., Feely, R. A., and Key, R. M. (2006), Global relationships of total alkalinity with salinity and temperature in surface waters of the world's oceans, Geophys. Res. Lett., 33, L19605, doi:10.1029/2006GL027207.

Olsen, A., et al: GLODAPv2.2019 – an update of GLODAPv2, Earth Syst. Sci. Data, 11, 1437–1461, https://doi.org/10.5194/essd-11-1437-2019, 2019

Olsen, A., et al.: GLODAPv2.2020 - the second update of GLODAPv2. Earth System Science Data Discussions, 1–41. https://doi.org/10.5194/essd-2020-165, 2020

Resplandy, L., Keeling, R. F., Rödenbeck, C., Stephens, B. B., Khatiwala, S., Rodgers, K. B., … Tans, P. P. (2018). Revision of global carbon fluxes based on a reassessment of oceanic and riverine carbon transport. *Nature Geoscience*, *11*(7), 504–509. https://doi.org/10.1038/s41561-018-0151-3

Sabine, C. L., et al. Surface Ocean CO2 Atlas (SOCAT) gridded data products, Earth Syst. Sci. Data, 5, 145–153, https://doi.org/10.5194/essd-5-145-2013, 2013.

2.2 Update of MPI-SOMFFN and new MPI-ULB-SOMFFN-clim

The Max Planck Institute for Meteorology Self-Organizing Map Feed Forward neural network (MPI-SOMFFN) method provides an estimate of the surface ocean partial pressure of CO_2 (pCO_2) and the contemporary air-sea CO2 flux for the period 1982-2019 for the open ocean. While this method has been established in the past [Landschützer et al 2013], it has - as part of the 4C project - been extended to the year 2019 [Friedlingstein et al 2020] and it will be further annually updated throughout this project. While MPI-SOMFFN only covers the open ocean, neglecting marginal seas and coastal oceans, a new constraint building on the SOMFFN method has been established under the umbrella of the 4C project, namely the Max Planck Institute for Meteorology and University of Brussels Self-Organizing Map Feed Forward neural network climatology (MPI-ULB-SOMFFN-clim) data product [Landschützer et al 2020]. This new pCO_2 climatology now covers large previously missing oceanic regions such as the Arctic Ocean, marginal seas and coastal oceans to provide a complete picture of the contemporary marine air-sea CO_2 exchange and has been created by merging the open ocean MPI-SOMFFN product with the coastal ocean SOMFFN based-product by Laruelle et al [2017].

2.2.1 Observations

Both MPI-SOMFFN and MPI-ULB-SOMFFN-clim are built from the gridded observations provided by the Surface Ocean CO_2 Atlas (SOCAT, [Bakker et al 2016, Sabine et al 2013]), i.e. the largest collection of quality-controlled surface ocean CO_2 measurements. While open ocean measurements are available on a 1° longitude by 1° latitude regular grid, coastal ocean observations are finer resolved with a resolution of 0.25° x 0.25°. SOCAT reports the fugacity of CO_2 (fCO_2), hence the respective observations have been converted to pCO_2 following Dickson et al [2007]. MPI-SOMFFN builds on measurements collected during the 1982-2019 period, whereas MPI-ULB-SOMFFN-clim largely builds on measurements collected throughout a narrower timeframe, i.e. between 1998 and 2015, due to the climatological nature of the product.

2.2.2 Method

The SOMFFN method consists of a 2-step approach that first uses a neural network-based clustering algorithm (SOM) to divide the ocean into biogeochemical provinces of similar carbon dynamics. In a second step a non-linear neural network regression method (FFN) establishes a relationship between auxiliary driver data from various observing platforms (e.g. satellite missions). The open ocean SOMFFN application uses 16 biogeochemical regions in the SOM step, with 1 additional biogeochemical region covering the Arctic ocean (MPI-ULB-SOMFFN-clim only) and the coastal ocean SOMFFN uses 10 biogeochemical regions. The respective FFN uses a set of environmental predictors (see Landschützer et al [2020] for more detail for both the open ocean and the coastal ocean) to establish a relationship between driver data and the SOCAT observations which is then further used to estimate the pCO2 from the same environmental drivers, where no measurements exist. To create the MPI-ULB-SOMFFN-clim product, open ocean and coastal ocean pCO_2 have been merged at their common geographical overlap areas.

2.2.3 Results

From the two products (MPI-SOMFFN and MPI-ULB-SOMFFN-clim) two distinct results emerged: Since a reduction/stagnation of the air-sea CO2 uptake occurred in the 1990´s, the global ocean has continuedly started to increase to annual mean rate at which carbon is absorbed, according to the new update of the MPI-SOMFFN product. 2019 was the year with the strongest carbon uptake since the beginning of the record in 1982 with an annual mean contemporary CO2 uptake of 2.2 Pg C yr-1. Since 2009 though, the increase in the annual carbon uptake significantly slowed down (0.3 Pg C yr-1 decade-1) in comparison to the 2000-2009 period (0.9 Pg C yr-1 decade-1). Adding a river flux correction of 0.78 Pg C yr-1 [Resplandy et al 2018] suggests an annual uptake of anthropogenic carbon of roughly 3 Pg C yr-1 in 2019.

Integrating the coastal oceans, the Arctic Ocean and marginal seas in MPI-ULB-SOMFFN, reveals that the aquatic continuum (the pCO2 from the coast to the open ocean) is well represented in the mid latitudes with differences in the common overlap area below 5% of the climatological mean pCO_2, but substantial mismatches

exist, particularly in seasonally ice-covered regions and in data-sparse regions such as the Peruvian upwelling system or the Arabian Sea where differences exceed 10% of the annual mean pCO_2. This mismatch is one order of magnitude larger as the current measurement uncertainty (<5 µatm), hence the observed strong gradients between the coast and the open ocean illustrate that more measurements are required to resolve the complex biogeochemical dynamics of these regions.

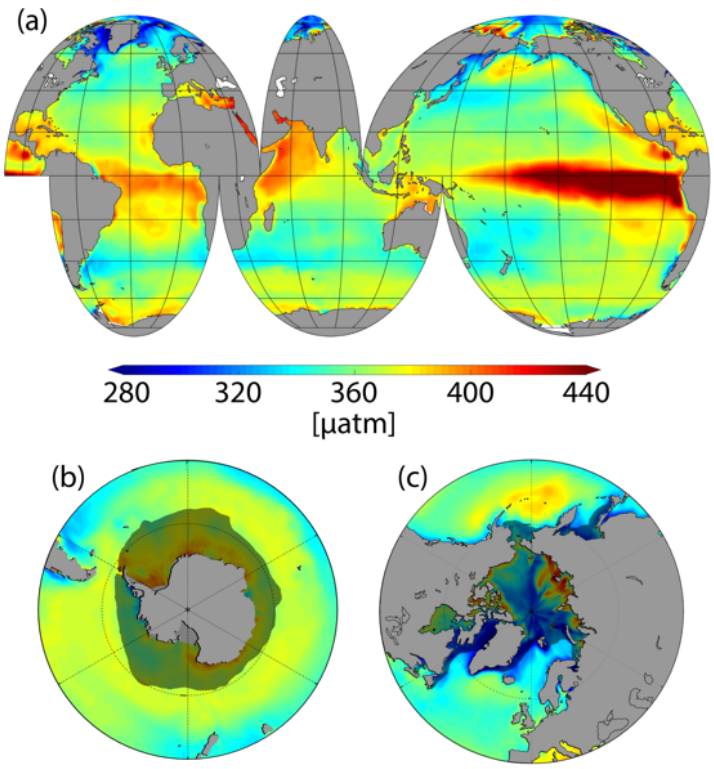

Figure 2: Climatological mean sea surface partial pressure of CO_2 from the MPI-ULB-SOMFFN-clim product covering open ocean as well as coastal ocean regions and marginal seas

2.2.4 Data availability

Both Products are published and publicly available. The MPI-SOMFFN product and its future annual updates are available from: https://www.ncei.noaa.gov/access/ocean-carbon-data-system/oceans/SPCO2_1982_present_ETH_SOM_FFN.html

The MPI-ULB-SOMFFN-clim product is equally published and available from: https://www.ncei.noaa.gov/access/ocean-carbon-data-system/oceans/MPI-ULB-SOM_FFN_clim.html

2.2.5 References

Bakker, D. C. E., et al.: A multidecade record of high-quality fCO2 data in version 3 of the Surface Ocean CO2 Atlas (SOCAT), Earth Syst. Sci. Data, 8, 383– 413, https://doi.org/10.5194/essd-8-383 2016, 2016.

Friedlingstein et al: Global Carbon Budget 2020, ESSD, in rev.

Landschützer, P., Laruelle, G. G., Roobaert, A., and Regnier, P.: A uniform pCO2 climatology combining open and coastal oceans, Earth Syst. Sci. Data, 12, 2537–2553, https://doi.org/10.5194/essd-12-2537-2020, 2020

Landschützer, P., Gruber, N., Bakker, D. C. E., Schuster, U., Nakaoka, S., Payne, M. R., Sasse, T. P., and Zeng, J.: A neural network-based estimate of the seasonal to inter-annual variability of the Atlantic Ocean carbon sink, Biogeosciences, 10, 7793–7815, https://doi.org/10.5194/bg-10-7793-2013, 2013

Laruelle, G. G., Landschützer, P., Gruber, N., Tison, J.-L., Delille, B., and Regnier, P.: Global high-resolution monthly pCO2 climatology for the coastal ocean derived from neural network interpolation, Biogeosciences, 14, 4545–4561, https://doi.org/10.5194/bg-14-4545-2017, 2017.

Resplandy, L., Keeling, R. F., Rödenbeck, C., Stephens, B. B., Khatiwala, S., Rodgers, K. B., … Tans, P. P. (2018). Revision of global carbon fluxes based on a reassessment of oceanic and riverine carbon transport. *Nature Geoscience*, *11*(7), 504–509. https://doi.org/10.1038/s41561-018-0151-3

Sabine, C. L., et al. Surface Ocean CO2 Atlas (SOCAT) gridded data products, Earth Syst. Sci. Data, 5, 145–153, https://doi.org/10.5194/essd-5-145-2013, 2013.

3 New observation-based constraints on interior carbon

3.1 Updating the global ocean anthropogenic carbon sink estimate based on the eMLR(C*) approach

Recently, the eMLR(C*) approach was developed [Clement and Gruber, 2018], which allows us to determine the change in anthropogenic carbon content, ΔC_{ant}, in the ocean interior through comparison of multiple linear regression (MLR) models fitted to observations from two subsequent time periods. Applying this method, Gruber et al. [2019] found that the ocean carbon sink had increased by 34 ± 4 petagrams of carbon (Pg C) between 1994 and 2007, which is equivalent to an average uptake rate of 2.6 ± 0.3 Pg C yr^{-1} and represents 31 ± 4% of the global anthropogenic CO_2 emissions over this period. It should be noted that 1994 and 2007 are the median years of two compared eras, namely the JGOFS/WOCE (1982-2000) and GO-SHIP (2000-2012) era. In the framework of 4C, we aim to update this estimate for newly available observations extending until 2019 [Olsen et al., 2020], as well as modify the method to derive information that is most useful as a constraint for modeling results.

3.1.1 Observations

The presented update of the ΔC_{ant} estimate was based on the latest release of the Global Ocean Data Analysis Project GLODAPv2_2020 [Olsen et al., 2020], which contains seven years of additional hydro-chemical observations from research vessel cruises that were not ingested in previous ΔC_{ant} estimates. The mapping of global ΔC_{ant} fields relies on predictor variable climatologies, namely the latest version of the World Ocean Atlas 2018 [Locarnini et al., 2019; Zweng et al., 2019], as well as the GLODAPv2 climatology [Lauvset et al., 2016].

3.1.2 Method

In brief, the eMLR(C*) method relies on the fitting MLR models to C* observations from two adjacent eras. C* is a conservative tracer of anthropogenic carbon derived from measured dissolved inorganic carbon by subtracting the imprint of organic matter remineralization and calcium carbonate dissolution. MLR models are fitted for all possible combinations of the following 7 independent variables: temperature, salinity, phosphate, silicic acid, $PO_4^* = PO_4 - 16 \cdot NO_3 + 2.9$, oxygen, and AOU under the constraint that a minimum of two, but not more than 5 independent tracers are selected. The coefficients of the ten MLR models with the lowest combined root mean squared error are than applied to the climatological data sets referenced above, to map ΔC_{ant} for the eras of interest. For additional details please refer to [Clement and Gruber, 2018; Gruber et al., 2019].

3.1.3 Results

Applying the eMLR(C*) method and comparing the 2000-2012 GO-SHIP era [Gruber et al., 2019] to the new era covering the years 2013-2019, we found an increase of the anthropogenic CO_2 sink of ~24 Pg C, which refers to the change between the median reference years 2007 - 2015. This is equivalent to an average uptake rate of 3.0 Pg C yr^{-1}. Assuming an uncertainty in the order of ± 0.3 Pg C yr^{-1} as estimated by Gruber et al. (2019), our average uptake rate is in agreement with the rate of 2.5 ± 0.6 Pg C yr^{-1} reported in the latest Global Carbon Budget for the period 2009 - 2018 [Friedlingstein et al., 2019]. The horizontal and vertical distribution of ΔC_{ant} (Fig. 1 and 2) is similar to that found in the previous analysis of the 1994 – 2007 period [Gruber et al., 2019]. However, the absolute numbers are lower, mainly due to the shorter reference period of 8 instead of 13 years.

It should be noted that a higher uncertainty must be expected for the new estimate, but has not yet been scrupulously determined. The main reason for the expected higher uncertainty is the lower data coverage, due to the shorter observational time period and the less dense sampling network. A comprehensive uncertainty assessment based on synthetic data from an hindcast ocean biogeochemical model [Clement and Gruber, 2018] is in preparation, but not yet finalized. Readjustment of the compared time slices will be considered to improve statistical robustness, and interpretability of findings as constraint for model-based and surface flux estimates.

.

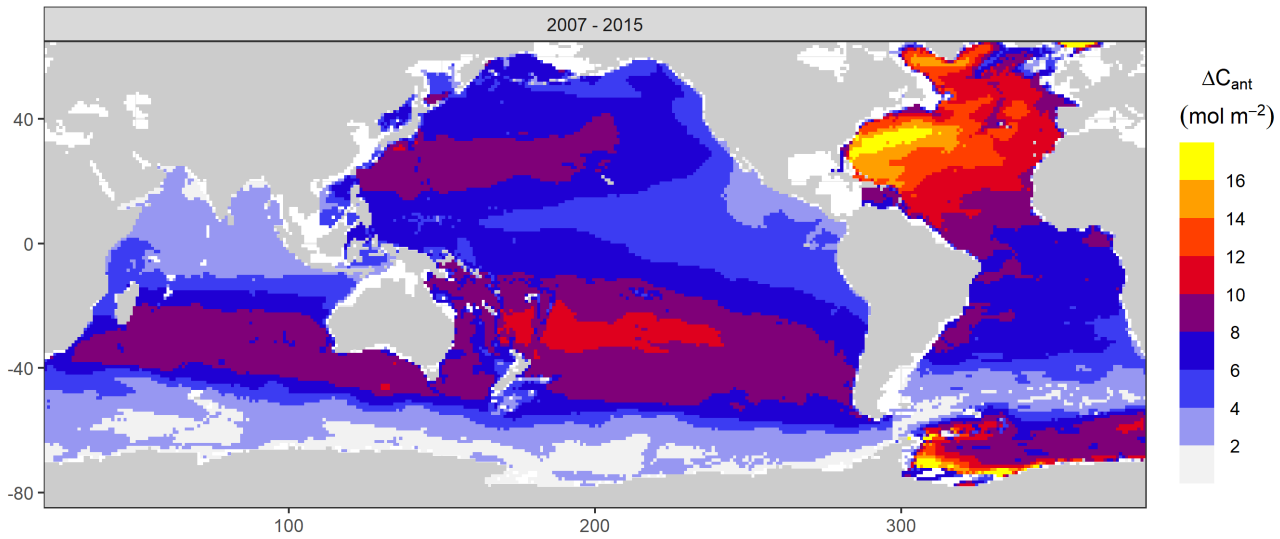

Figure 3: Map of the column inventory of anthropogenic CO_2 in the ocean (0 to 3000 m) between 2007 and 2015 based on the eMLR(C*) method.

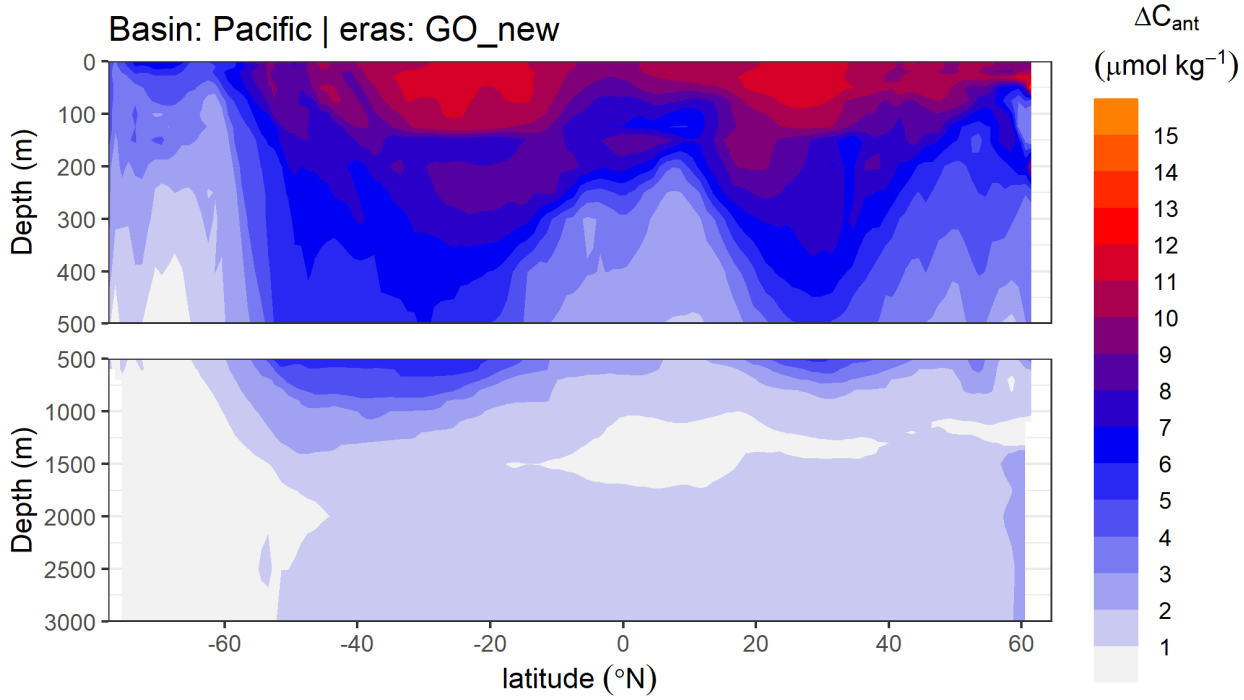

Figure 4: Zonal mean section of the change in anthropogenic CO_2 between 2007 and 2015 in the Pacific Ocean. The upper 500 m are expanded.

3.1.4 Data availability

Results from the previous study [Gruber et al., 2019] covering the 1994-2007 period are available at:

https://www.ncei.noaa.gov/access/ocean-carbon-data-system/oceans/ndp_100/ndp100.html

Updated results for the 2007 – 2015 period will be made available upon request (contact: jensdaniel.mueller@usys.ethz.ch).

3.1.5 References

Clement, D. and Gruber, N.: The eMLR(C*) Method to Determine Decadal Changes in the Global Ocean Storage of Anthropogenic CO 2, Global Biogeochem. Cycles, 32(4), 654–679, doi:10.1002/2017GB005819, 2018.

Gruber, N., Clement, D., Carter, B. R., Feely, R. A., van Heuven, S., Hoppema, M., Ishii, M., Key, R. M., Kozyr, A., Lauvset, S. K., Lo Monaco, C., Mathis, J. T., Murata, A., Olsen, A., Perez, F. F., Sabine, C. L., Tanhua, T. and Wanninkhof, R.: The oceanic sink for anthropogenic CO2 from 1994 to 2007, Science, 363(6432), 1193–1199, doi:10.1126/science.aau5153, 2019.

Lauvset, S. K., Key, R. M., Olsen, A., van Heuven, S., Velo, A., Lin, X., Schirnick, C., Kozyr, A., Tanhua, T., Hoppema, M., Jutterström, S., Steinfeldt, R., Jeansson, E., Ishii, M., Perez, F. F., Suzuki, T. and Watelet, S.: A new global interior ocean mapped climatology: the 1◦ × 1◦ GLODAP version 2, , 16, 2016.

Locarnini, R., Mishonov, A., Baranova, O., Boyer, T., Zweng, M., Garcia, H., Reagan, J., Seidov, D., Weathers, K., Paver, C., Smolyar, I. and Locarnini, R.: World Ocean Atlas 2018, Volume 1: Temperature., 2019.

Olsen, A., Lange, N., Key, R. M., Tanhua, T., Bittig, H. C., Kozyr, A., Àlvarez, M., Azetsu-Scott, K., Becker, S., Brown, P. J., Carter, B. R., Cotrim da Cunha, L., Feely, R. A., van Heuven, S., Hoppema, M., Ishii, M., Jeansson, E., Jutterström, S., Landa, C. S., Lauvset, S. K., Michaelis, P., Murata, A., Pérez, F. F., Pfeil, B., Schirnick, C., Steinfeldt, R., Suzuki, T., Tilbrook, B., Velo, A., Wanninkhof, R. and Woosley, R. J.: GLODAPv2.2020 – the second update of GLODAPv2, preprint, Oceanography – Chemical., 2020.

Zweng, M. M., Reagan, J., Seidov, D., Boyer, T., Locarnini, R., Garcia, H., Mishonov, A., Baranova, O. K., Paver, C. and Smolyar, I.: WORLD OCEAN ATLAS 2018 Volume 2: Salinity., 2019.

3.2 MOBO-DIC_MPIM

The seasonal cycle represents one of the largest signals of the natural carbon cycle in the ocean. Yet, the seasonal pattern of dissolved inorganic carbon (DIC) is not well established at a global scale. Here, we present a monthly climatology of Mapped Observation-Based Oceanic DIC by the Max-Planck-Institute for Meteorology (MOBO-DIC_MPIM_monthly-clim), extending from 65°N to 65°S, from the surface to 2000 m.

On longer timescales, the oceanic uptake of carbon dioxide (CO_2) from the atmosphere is highly variable. However, it is unclear how this variability and trend is reflected in the DIC pool. To investigate the trend and interannual variability of DIC, we increased the temporal resolution of MOBO-DIC_MPIM, providing monthly fields of DIC from 2004 through 2018, in the upper ocean until 500 m (MOBO-DIC_MPIM_2004-2018).

3.2.1 Observations

The monthly climatology is based on shipboard measurements of DIC, from the GLobal Ocean Data Analysis Project Version 2.2019 [Olsen et al 2019]. We use the gridded GLODAP data of DIC on a 1°x1° grid from 2004 through 2017, in the upper ocean until 2000 m from 65°N to 65°S.

Our estimate at monthly resolution is based on GLODAPv2.2020 data on a 1°x1° grid from 2004 through 2018 [Olsen et al., 2020], in the upper ocean until 500 m, from 65°N to 65°S, and in addition, extends until 80°N in the Atlantic.

3.2.2 Method

We apply and extend the SOM-FFN approach described in Section 2.2 to obtain time-varying gap-filled mapped fields of DIC in the water column. We adjusted the SOM-FFN method in several ways compared to the original method by Landschützer et al. [2013], which mapped oceanic surface pCO_2. As we map the DIC in the water column, we extend the mapping grid from three dimensions (latitude, longitude, and time), to four (latitude, longitude, time, and depth). As different predictors are available and/or meaningful when mapping DIC in the water column, we also have a different set of predictor data compared to the approach used by Landschützer et al. [2013].

For the full description of the method and its validation, please refer to both the Main Text and the Supporting Information of Keppler et al. [2020a, in review at GBC] and for the dataset please see Keppler et al. [2020b].

3.2.3 Results

Surface DIC maxima occur in hemispheric spring, and minima in fall, driven by the input of DIC into the upper ocean by mixing during winter, and net community production (NCP) driven draw-down of DIC over summer. The seasonal pattern seen at the surface extends to a nodal depth of <50 m in the tropics and several hundred meters in the subtropics. Below the nodal depth, the seasonal cycle of DIC has the opposite phase, primarily owing to the seasonal accumulation of DIC stemming from the remineralization of sinking organic matter. The well captured seasonal draw-down of DIC in the mid-latitudes (23° to 65°) allows us to estimate the spring-to-fall NCP in this region. We find a spatially relatively uniform spring-to-fall NCP of 1.9±1.3 mol C m^{-2} yr^{-1}, which sums to 3.9±2.7 Pg C yr^{-1} over this region. This corresponds to a global spring-to-fall NCP of 8.2±5.6 Pg C yr^{-1}.

In contrast to the seasonal climatology, interannual variations have not been fully scrutinized. However, first results reveal some expected features. Based on the monthly fields from 2004 through 2018, we find the largest interannual variability at the surface of the tropical Pacific linked to the El Nino Southern Oscillation. The oceanic DIC concentration is increasing almost everywhere, with the largest positive trend at the surface in the tropical West Pacific. Concurrently, the Southern Ocean has a comparatively weak trend particularly in upwelling regions. Overall, we find a global mean increase in the surface ocean DIC of 9 µmol kg^{-1} $decade^{-1}$.

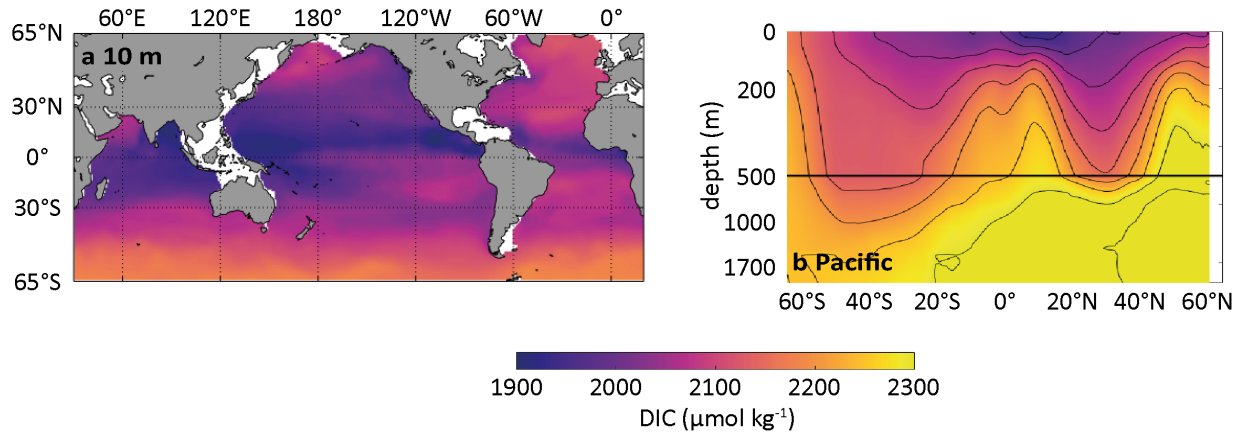

Figure 5: Temporal mean of MOBO-DIC_MPIM (monthly-clim) (a) Map of the annual mean DIC concentration at 10 m. (b) Vertical zonal section of the mean DIC in the Pacific. Zoomed in to the top 500 m (delimited in black). Black contour lines are drawn every 50 µmol kg^{-1}.

The monthly climatology of MOBO-DIC_MPIM is freely available to the public from NCEI/OCADS [Keppler, et al., 2020b, https://www.ncei.noaa.gov/access/ocean-carbon-data-system/oceans/ndp_104/ndp104.html].

The monthly fields from 2004 through 2018 are currently in the final testing stage, before being submitted to NCEI/OCADS.

3.2.4 References

Keppler, L. Landschützer, P., Gruber, N. Lauvset, S.K. and Stemmler, I.: Seasonal carbon dynamics in the near-global ocean, Global Biogeochemical Cycles, in rev. 2020a

Keppler, L. Landschützer, P., Gruber, N. Lauvset, S.K. and Stemmler, I.: Mapped Observation-Based Oceanic Dissolved Inorganic Carbon (DIC), monthly climatology, from January to December (based on observations between 2004 and 2017), from the Max-Planck-Institute for Meteorology (MOBO-DIC_MPIM) (NCEI Accession 0221526). NOAA National Centers for Environmental Information. Dataset. https://doi.org/10.25921/yvzj-zx46, 2020b

Landschützer, P., Gruber, N., Bakker, D. C. E., Schuster, U., Nakaoka, S., Payne, M. R., Sasse, T. P., and Zeng, J.: A neural network-based estimate of the seasonal to inter-annual variability of the Atlantic Ocean carbon sink, Biogeosciences, 10, 7793–7815, https://doi.org/10.5194/bg-10-7793-2013, 2013

Olsen, A. et al.: GLODAPv2.2019 – an update of GLODAPv2. Earth System Science Data, 11(3), 1437–1461. https://doi.org/10.5194/essd-11-1437-2019, 2019

Olsen, A., et al.: GLODAPv2.2020 - the second update of GLODAPv2. Earth System Science Data Discussions, 1–41. https://doi.org/10.5194/essd-2020-165, 2020